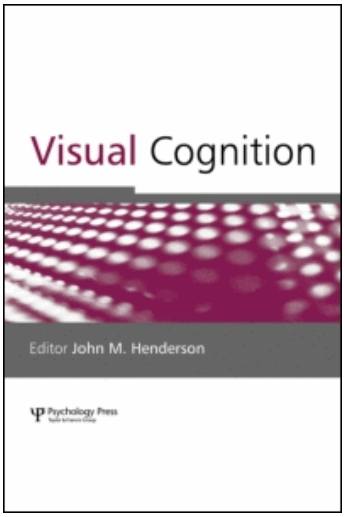

Visual Cognition
Publication details, including instructions for authors and subscription information:
http://www.informaworld.com/smpp/title~content=t713683696

Identification of fragmented object outlines: A dynamic interplay between different component processes

Katrien Torfs[a]; Sven Panis[a]; Johan Wagemans[a]
[a] Laboratory of Experimental Psychology, University of Leuven, Leuven, Belgium

First published on: 12 July 2010

To cite this Article Torfs, Katrien , Panis, Sven and Wagemans, Johan(2010) 'Identification of fragmented object outlines: A dynamic interplay between different component processes', Visual Cognition, 18: 8, 1133 — 1164, First published on: 12 July 2010 (iFirst)
To link to this Article: DOI: 10.1080/13506281003693593
URL: http://dx.doi.org/10.1080/13506281003693593

VISUAL COGNITION, 2010, 18 (8), 1133–1164

Psychology Press
Taylor & Francis Group

Identification of fragmented object outlines: A dynamic interplay between different component processes

Katrien Torfs, Sven Panis, and Johan Wagemans

Laboratory of Experimental Psychology, University of Leuven, Leuven, Belgium

The speed of fragmented picture identification depends on a large number of factors whose effects might change in time during an identification attempt. Using survival analysis and fixed fragmentation levels, previous research has shown that effects of complexity, fragment curvature, and time interact. Here, we study the effects of presentation duration and dynamic fragmentation levels. Fragmented object outlines were presented repetitively every 2.25 s, and at each presentation longer fragments were shown (possibly until closure). We recorded the lowest presentation number (minimum 1, maximum 10) that resulted in correct naming by the participants ($N = 84$). Survival analysis was employed to investigate whether and when different factors like presentation duration, complexity, object category (natural vs. artifactual), symmetry, proximity, and fragment curvature influence correct identification. The results confirm and extend previous findings, and are interpreted within a dynamic, interactive processing framework.

Keywords: Contour integration; Curvature singularities; Fragmented pictures; Grouping; Interactive processing; Matching; Object identification; Survival analysis.

The perceptual information value of various segments or points of the contour of an object has been the interest of many researchers (e.g., Attneave, 1954; and more recently, e.g., Biederman, 1987; de Winter & Wagemans, 2008a; Feldman & Singh, 2005; Kennedy & Domander, 1985; Norman, Philips, & Ross, 2001). For example, a lot of research has been conducted to find out whether curved fragments are more important

Please address all correspondence to Johan Wagemans, Laboratory of Experimental Psychology, University of Leuven, Tiensestraat 102, B-3000 Leuven, Belgium. E-mail: johan.wagemans@psy.kuleuven.be

We would like to acknowledge support from long-term structural funding (METH/08/02) by the Flemish Government, awarded to JW. SP has a postdoctoral fellowship from the Fund for Scientific Research (FWO Flanders). We thank Jessica Bulthé and Joline Rediers for assistance with data collection.

http://www.psypress.com/viscog DOI: 10.1080/13506281003693593

compared to straight ones, but different stimuli and paradigms were used, leading to contradictory conclusions (for an overview, see Panis, de Winter, Vandekerckhove, & Wagemans, 2008). To study the role of curvature singularities in shape and object perception more systematically, we set up a rather extensive research programme consisting of a series of studies using different manipulations of the same large set of object contour stimuli (de Winter & Wagemans, 2004, 2006, 2008a, 2008b; Panis et al., 2008; Panis & Wagemans, 2009; Wagemans et al., 2008).

Panis and Wagemans (2009) investigated the effects of different factors on the time it takes to identify an object from its fragmented outline. They studied the dynamic interplay between the effects of category membership (natural vs. artifactual), visual shape complexity, fragment curvature (straight vs. curved), and configural properties (symmetry, proximity, collinearity) on two component processes involved in the identification of fragmented object outlines: The perceptual grouping of the fragments and the matching of the evolving structural representation to memory. A number of predictions concerning these effects were derived from multiple lines of research within the literature: (1) The configural properties between the fragments (symmetry, proximity, etc.), and not the local properties of the fragments (length, curvature, etc.) dominate early grouping processes; (2) visually complex shapes have a grouping disadvantage but a matching advantage, whereas simple shapes have a grouping advantage but a matching disadvantage; and (3) fragmented object outlines of natural categories are identified faster and/or more accurately compared to artifactual categories.

First, with fragmented object outlines, geometric extrapolation accuracy can be expected to be determined by the interaction between local fragment properties (absolute position, length, orientation, curvature) and configural, or nonaccidental properties between fragments (relative position or proximity, collinearity and curvilinearity, symmetry or parallelism, density, etc.). The visual system is organized hierarchically, with the lowest levels responding to simple features such as small oriented lines, intermediate levels to longer oriented lines and curved segments, and the highest levels to the shape and outline of objects and/or their parts. At each level, competitive grouping occurs based on well-established Gestalt principles such as proximity and collinearity at lower levels, and convexity relations and symmetry (Locher & Wagemans, 1993; Machilsen, Pauwels, & Wagemans, 2009; Nucci & Wagemans, 2007; Wagemans, 1992, 1993, 1995, 1997) at higher levels. This competition is mediated by horizontal connections at each level with the strongest groupings being fed back to lower levels where they contextually constrain the ongoing competitive representations of the input. For example, during grouping, global convexity relations between contour segments at higher levels can override local good continuation and relatability of fragments at lower levels (Liu, Jacobs, & Basri, 1999). Thus,

due to interactions between levels, visual processing at each level is influenced by bottom-up image-based geometric characteristics as well as by top-down influences (Kimchi & Hadad, 2002; Lamme, Supèr, & Spekreijse, 1998; Murray, Schrater, & Kersten, 2004). Kimchi and Bloch (1998) have suggested that when both local properties and global properties are present in the stimuli and when both can be used for the task, global properties (the configural relations between fragments) dominate early completion processes, and not the local fragment properties such as curvature (see also Schendan & Kutas, 2007; Sekuler, Palmer, & Flynn, 1994; Spillman, 1999). Note that configural properties can be local (e.g., proximity between two neighbouring fragments on the contour) or more global (convexity relations between larger curved segments).

Second, it has been suggested that the system first uses coarse, global information contained in low spatial frequencies to reduce the number of different activated candidate object representations, and to guide the incoming information about the local properties or details which is only available later when focused attention is directed to it (Bar, 2003; Hochstein & Ahissar, 2002; Sanocki, 1993, 2001; Schendan & Kutas, 2002, 2007). For example, Sugase, Yamane, Ueno, and Kawano (1999) showed that object-selective VOT neurons first convey global, categorical information before they convey local, fine identity information. Also, the results of a combined fMRI-MEG study using masked object pictures as stimuli (Bar et al., 2006) suggested that only the low spatial frequencies in an object image are projected quickly from V1 to VOT and prefrontal areas where they activate the long-term memory visual and semantic representations of candidate objects. These triggered memory representations generate object-based expectancies that are then top-down projected to the rest of the visual cortex (see also Kosslyn et al., 1994; Kveraga, Boshyan, & Bar, 2007; Tomita, Ohbayashi, Nakahara, Hasegawa, & Miyashita, 1999). These expectancies will match or mismatch with more detailed information represented in lower levels, and allow the rejection of incorrect candidates.

Now, because shapes with a low visual complexity have a high a priori probability of occurrence and vice versa (Donderi, 2006), we cannot only expect that fragmented outlines of low complex shapes are a priori easier to group (bottom-up), but also that they will activate a larger number of (previously experienced) candidate objects early in processing compared to high complex shapes, and that later interactive top-down guided matching processes will therefore last longer. Conversely, fragmented outlines of high complex shapes are a priori more difficult to group, and, once grouped correctly, will activate few candidate objects resulting in fast matching.

Third, Gerlach and colleagues (Gerlach et al., 2002; Gerlach, Law, & Paulson, 2004, 2006) have suggested that the structural similarity between stored exemplars of different categories affects the matching and the

grouping processes that are required to access a stored object shape representation in a different way. High structural similarity between stored exemplars is advantageous for integrating local object features into whole object representations because the global and local features of these exemplars are more stable and more highly correlated than the features of exemplars from categories with low structural similarity. At the same time, however, high structural similarity is harmful for matching operations, because there will be more competition between activated candidate object representations delaying covert identification.

As a result, under optimal grouping conditions (i.e., with complete line drawings and unlimited exposure), objects with low structural similarity (e.g., artifactual objects) are named faster and more accurately because there is less competition at the level where activated object representations compete for selection (a matching advantage), compared to objects with high structural similarity (e.g., natural objects). In contrast, under sub-optimal grouping conditions (i.e., fragmentation and/or limited exposure duration), natural objects can be named faster and more accurately (Gerlach et al., 2002, 2004, 2006). This happens because (1) under such conditions task performance tends to depend on global shape information carried by low spatial frequencies, and (2) outlines and silhouettes of natural objects are better identifiable than those of artifacts, because the global shape of natural objects might contain more salient features or less 2-D/3-D ambiguity (Lloyd-Jones & Luckhurst, 2002; Wagemans et al., 2008), whereas artifacts are believed to rely more on a part-based structural description (Riddoch & Humphreys, 2004). Thus, because difficult grouping processes can be influenced by early feedback information from activated object representations, the global shape characteristics of activated candidate natural object representations produce a grouping advantage under sub-optimal grouping conditions, which can outweigh their disadvantage during matching, relative to artifactual objects (Gerlach et al., 2002, 2004, 2006; Humphreys & Forde, 2001; Humphreys, Riddoch, & Quinlan, 1988).

A fourth prediction tested by Panis and Wagemans (2009) was that the perceptual information value of straight and curved contour segments changes over time depending on visual complexity, as predicted by Panis et al. (2008). Specifically, straight segments of a contour play a larger role for complex object outlines (with high part saliency) during early grouping processes, whereas curved segments of object outlines are more important during later matching processes for simpler outlines (with low part saliency). Simpler outlines—where grouping of fragments (regardless of their curvature) will quickly lead to the correct global shape—will activate many candidate objects, and curved segments contain much more information about part boundaries and protrusions (Biederman, 1987) to exclude incorrect candidates during the top-down matching process, compared to

straight segments. In contrast, because Singh and Fulvio (2005) found an extrapolation cost for curvature (straight segments convey more direction information compared to curved segments of the same length), the probability of a correct grouping of the fragments of complex shapes is higher with straight compared to curved fragments. Furthermore, once grouped correctly, the global shape of a visually complex object outline can be matched quickly to memory.

Panis and Wagemans (2009) were able to confirm these predictions using a discrete-identification paradigm in which the masked presentation duration of 20% fragmented object outlines was repeatedly increased until correct naming occurred. Discrete time survival analysis was applied to allow investigating whether, and if so, when different types of information such as contour integration cues (proximity and collinearity), fragment properties (low vs. high curvature), stimulus complexity, global symmetry, and object category (natural vs. artifactual) influenced correct identification.

The main goals of the present study were to study the effect of exposure duration, and to see which effects obtained by Panis and Wagemans (2009) can be replicated using a dynamic build-up paradigm with fragments increasing in length in 10 steps, starting with 10% of the contour until the contour is closed (100%). Although the presentation duration increased with repetitions of the same (masked) fragmented outline in Panis and Wagemans' study, we now used constant presentation times for each stimulus. Furthermore, each stimulus was presented to an observer for either 1000 ms (and not masked), or for 150 ms (and masked). The stimulus set consisted of 150 intact object outlines as well as fragmented versions (nine deletion levels, and two fragment types: Low or high curvature). We recorded the lowest presentation number (1–10) that resulted in correct naming by the participants.

We can expect a number of different results compared to Panis and Wagemans (2009). First, with fragments increasing in size, the average gap length across neighbouring fragments will decrease (increasing proximity), and grouping will become less and less ambiguous (less incorrect groupings). We can therefore expect that the hazard probability of correct identification will increase steadily across time (i.e., across presentations of the same object). Because Panis and Wagemans used a single fragmentation level during each presentation (80% contour-deleted outlines), the proximity value was constant across time for every object (as was the case for the values of other predictors). Here, proximity increases with each repetition for every object (when measured as average gap length, it decreases with each repetition). Survival analysis can handle such a "time-varying" predictor.

Second, when fragments increase in size, the positive effect of (small) straight fragments on early grouping for complex object outlines, and the positive effect of (small) curved fragments during later matching for simple

object outlines are both expected to be decreased, or even absent, because the perceptual distinction becomes less and less clear when fragments grow longer (small straight fragments become curved; small curved fragments start to include straight segments).

Discrete time survival analysis (Allison, 1982; Panis & Wagemans, 2010; Singer & Willett, 1993, 2003) is used to investigate whether and when predictors such as exposure duration, fragment properties (low vs. high curvature), configural properties (proximity, symmetry), stimulus complexity, and object category (natural vs. artifactual) influenced the timing of correct identification at the basic level. Survival analysis is a statistical technique to analyse time-to-event data, that is, data about the time between a well-defined starting point (in this case, the onset of the first presentation) and the occurrence of a target event (in this case, correct identification). Here, we measure time in discrete units of 2.25 s (the stimulus onset asynchrony between two subsequent presentations), which gives rise to interval-censored data (we only know that correct identification occurred somewhere between the onsets of two subsequent presentations) or right-censored data. Right-censored observations are trials in which a subject does not identify the object correctly after the final (tenth) presentation. These trials are not ignored in a survival analysis because they indicate that the event did not occur during the data collection period.

The quantity of interest in a survival analysis is hazard. When we treat our time-to-event data as observations of a discrete random variable T, one usually characterizes T by its probability mass function or $P(T = t)$, or its cumulative distribution function or $P(T \leq t)$. Two other mathematically—but not subjectively—equivalent ways are the hazard and survivor function (Luce, 1986). Discrete time hazard is defined as the probability that the event will occur in discrete time bin t given that the event did not occur in a previous time bin, or $P(T = t|T \geq t)$. The survivor function or $P(T > t)$ gives the probability that the event will occur later than time bin t. In contrast to the probability mass function which assesses the probability of event occurrence at the starting point of time, that is, when events still can occur at any time, the hazard function assesses the probability of event occurrence at each (discrete) time point t given that the event has not occurred before, that is taking into account the passage of time. For example, assume a dynamic system that can output events at three equally likely discrete points in time, $t1 < t2 < t3$. At Time 0 the probability (mass) at each time point equals 1/3, but if we observe that the event did not occur at time point 1, then the hazard probability (or the risk or instantaneous tendency) of event occurrence at time point 2 equals ½. Similarly, when the event did not occur at time points 1 and 2, the hazard at time point 3 equals 1. Although survival analysis can handle continuous time units (e.g., Cox regression), the estimation of the continuous time hazard functions is not straightforward

(Luce, 1986; Singer & Willett, 2003). There are a number of advantages to study hazard functions (e.g., compared to mean reaction times). Censored observations do not need to be ignored, the effect of time and time-varying effects of predictors can be studied, and discrete time hazard functions can be estimated without making any assumption about their shapes (Panis & Wagemans, 2010; Singer & Willett, 2003).

METHODS

Participants

Eighty-four subjects participated in this study (aged 17–26 years; 13 men). Seventy-eight subjects were first-year psychology students who participated as a mandatory component of their curriculum. The remaining subjects were students of other faculties. All participants reported normal or corrected-to-normal vision; they were unfamiliar with the stimuli, and naïve regarding the purpose of the study.

Stimuli

The stimulus set consisted of one intact outline and 18 fragmented versions for each of 150 objects. These outlines were derived from the large set of line drawings of everyday objects published by Snodgrass and Vanderwart (1980). Outlines were extracted from silhouettes, which in turn were created by filling-in the interior surfaces of the original line drawings. A more detailed description of outline construction can be found in Wagemans et al. (2008); see also de Winter & Wagemans, 2004; Panis & Wagemans, 2009; Wagemans, Notebaert, & Boucart, 1998).

For this study we selected 150 objects with high identification rates of the closed outlines, as determined in a large, normative study (Wagemans et al., 2008). This set included 84 artifactual objects (including vehicles, furniture, clothing, etc.) and 66 natural objects (including animals, fruits and vegetables, and body parts).

Two types of contour deletion were applied. Fragments were placed around the salient points (SPs; de Winter & Wagemans, 2008b; Panis et al., 2008), or around the midpoints (MPs, the contour points halfway in-between two SPs). Fragments placed around SPs result in curved fragments, and those placed around MPs result in relatively straight fragments. This is due to the fact that SPs typically have a large curvature value. We used these types of fragmentation because de Winter and Wagemans (2008b) have found that straight-line stimuli based on subjectively defined salient points were better identifiable than those based on mathematically defined extrema.

Instead of a linear increase of percentage contour shown in each trial, we calculated the percentage contour shown at each level x (x = 1, 2, ... 10) as 100 times alpha$^{(10-x)}$ (Snodgrass & Corwin, 1988). With alpha set to .77 (chosen to start the build-up process at 10%), this function resulted in the following percentages: 10, 12, 16, 21, 27, 35, 46, 59, 77, and 100 (the intact outline). Compared to a linear function, less perceptual information is added during early levels (and more later) to slow down the recognition process. The requested percentage contour shown at each level was approximated by starting from the relevant set of target points (i.e., SPs or MPs) and letting the fragments grow until the requested percentage was reached taking into account the distances along the contour between the target point and both of its neighbouring points. This procedure results in presenting the same number, and equally evenly distributed fragments for each fragmented version of an object outline. Examples of fragmented object outlines can be found in Figure 1.

Procedure

Stimuli were presented centred on a 17-inch CRT display with a refresh rate of 60 Hz and at a viewing distance of approximately 60 cm (viewing distance was not strictly controlled). The display resolution was set to 1024×768 pixels. Stimuli were all contained within a box of 640×480 pixels, resulting in a viewing angle of about 16×12 degrees. E-Prime (www.pstnet.com) was used to deliver presentation times at ms accuracy. All participants were tested individually.

A schematic presentation of the procedure is shown in Figure 2. Each trial consisted of one or more stimulus presentations of a fragmented version of the same object. Stimulus onset asynchrony was 2.25 s. These 2.25 s periods served as discrete time units used to measure the time it takes to identify the object. Trials were self-paced, starting with a fixation cross for 250 ms, and followed by an object outline at fragmentation level 1 (10% of the contour) in one of both fragmentation conditions (MP or SP). The object outline was presented for either 1000 ms or 150 ms. When presented for 150 ms, the object outline was followed by a random noise mask for 850 ms. A blank screen containing only a "?" was presented subsequently for 1000 ms. Participants were asked to press a button as soon as they believed they had identified the object in the dynamic stimulus. Only when a buttonpress was detected, the build-up process was interrupted, and the participant was asked to name the object aloud. The experimenter evaluated the response online (for the scoring specifications, see later). When the response was scored as correct, a new object outline (fragmentation level 1) was shown in the next trial. When the response was incorrect, the build-up

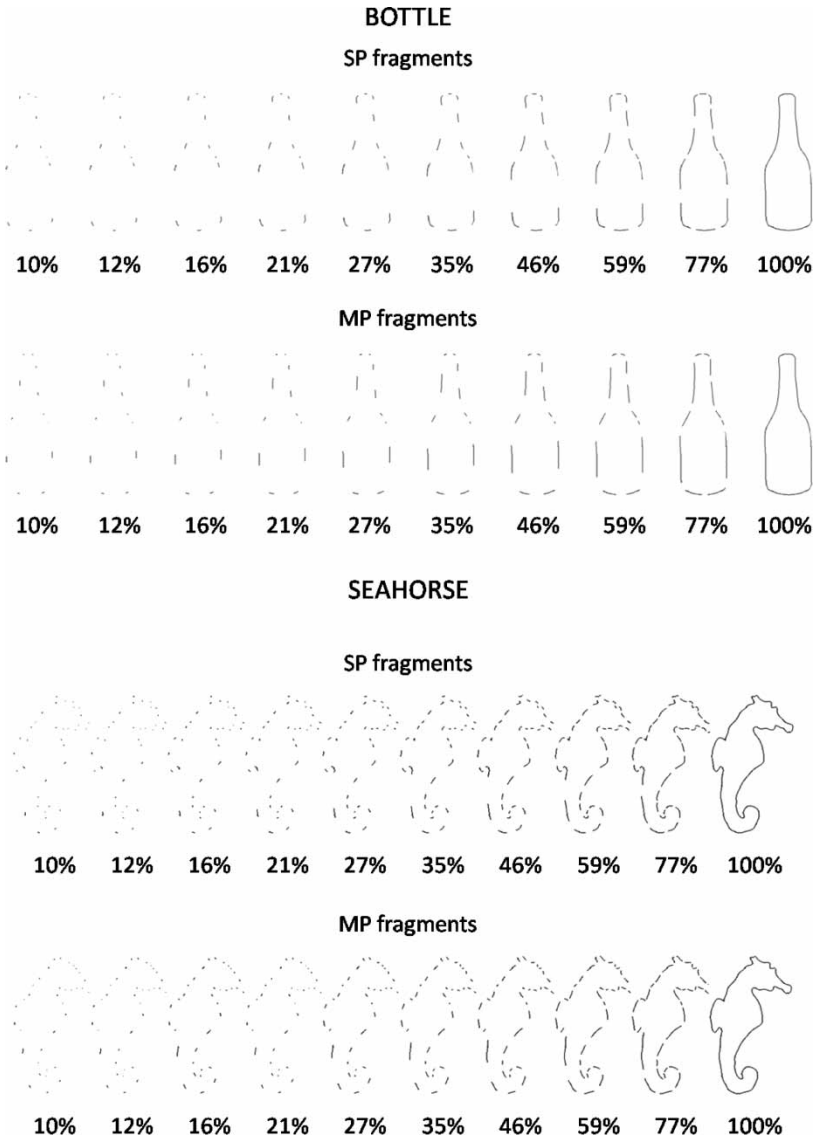

Figure 1. Example of fragmented outlines (bottle and seahorse) in two fragmentation types (SP and MP). Note that the stimuli in the experiment were presented in white on a black background.

process of the current outline continued (possibly showing 12%, 16%, 21%, 27%, 35%, 46%, 59%, 77%, and 100% of the contour). Participants were given feedback about the correctness of their answer and they were informed when a new object would appear. At the beginning of the experiment, there

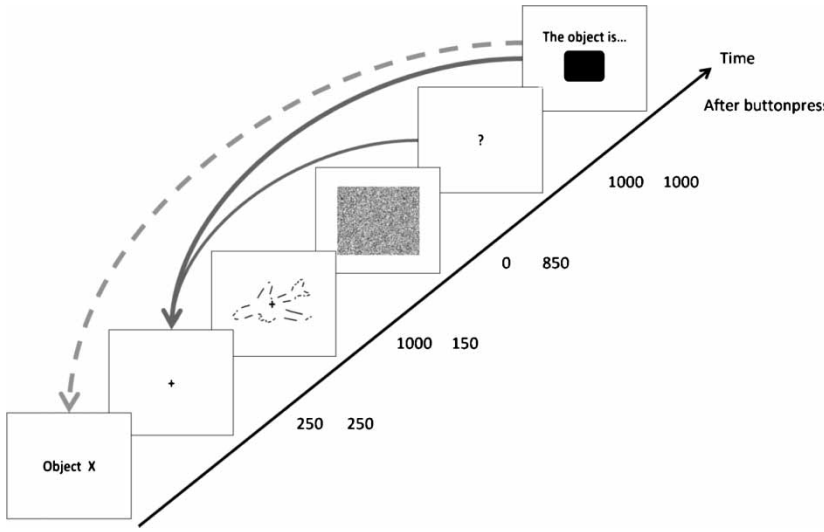

Figure 2. The dynamic build-up paradigm: Trials started with a 250 ms fixation cross, and were followed by a fragmented object outline presented for 1 s, or for 150 ms followed by a mask for 850 ms. When no response was registered at the end of a subsequent 1 s period showing a "?", the fixation cross reappeared and the build-up of the outline continued (small full grey arrow). When a response was registered but the answer was incorrect, then the build-up continued as well (large full grey arrow). When a correct response was given, the build-up of the current object outline was aborted, and the build-up of the next object started (dashed light grey arrow).

were some practice trials with a separate set of 10 objects (same set for all participants).

Half of the participants ($N = 42$) tried to identify MP fragmented versions of all objects; the other 42 participants saw the SP fragments of all object outlines. For half of the participants in each of these two groups, the presentation time of each fragmented object outlines was 1000 ms; this was 150 ms (followed by a mask for 850 ms) for the other half. The presentation order of the objects was randomized for each participant separately.

Scoring

In the present study, we used the same scoring rules as Panis and Wagemans (2009). A response was counted as correct when the same name was given as the one listed by Snodgrass and Vanderwart (1980). Because our participants were either Flemish or Dutch speaking, a synonym or dialect name that clearly indicated the same concept was also scored as correct. Severens, van Lommel, Ratinckx, and Hartsuiker (2005) have shown that Dutch (and

especially Flemish) has more synonyms, and dialect names than English. We also approved names referring to closely related objects if these were not visually distinguishable in the object outlines (e.g., "mouth" for "lips", "rat" for "mouse" or "cradle" for "baby carriage"). However, we did not allow slightly related names when they referred to different basic-level categories which are visually distinguishable in the object outlines (e.g., "shoe" and "boot" or "chicken" and "bird"). Scoring was done manually by the experimenter. Three experimenters were engaged in this study. Therefore, we used a scoring key based on a naming database from previous studies (e.g., de Winter & Wagemans, 2004). For each combination of object and participant, we recorded the lowest presentation number (1–10) that resulted in correct naming.

Survival analysis

Considering correct identification as the target event, trial onset as "the beginning of time", and the 2.25 s stimulus–onset asynchrony periods as discrete units to measure time, we can employ survival analysis to analyse our discrete time-to-event data (Singer & Willett, 1993, 2003). The 150 objects acted as experimental units, and the data of the participants were treated as repeated identifiability measures of the experimental units. An important aspect of this analysis is that it deals even-handedly with both observed and censored (i.e., nonoccurrence of the target event during data collection) event times. This is necessary because some outlines will never be identified correctly by participants during data collection.

The sample distribution of event occurrence is summarized by two statistics: The hazard function or $P(T = t|T \geq \mathrm{t})$ and the survivor function or $P(T > t)$. Whereas the hazard function assesses the unique risk of event occurrence associated with each time bin or time period of 2.25 s, the survivor function cumulates the bin-by-bin risks of event nonoccurrence and gives the probability that each time bin will "survive" event occurrence. Both functions need to be examined to identify the time bin in which most events have occurred.

Because the hazard function is bounded between 0 and 1, we need to apply a transformation before generalized linear models (GLM) for repeated measurements can be fitted to the data. As before (see Panis & Wagemans, 2009), we applied the nonlinear, asymmetric complementary log-log link function (cloglog hazard = ln(–ln(1–hazard))). This transformation is most attractive when discrete interval-censored data are collected due to data collection constraints (i.e., we know that identification occurred somewhere during a trial; Singer & Willett, 2003).

Discrete time hazard modelling

To explain why events occur at different time periods for different types of trials and/or different subjects, discrete-time hazard models must be fitted to the data. By specifying a hazard model, you make hypotheses about how you think different predictors (including time) are related to the risk of event occurrence in each time bin. When we analyse RTs with ANOVA, we treat time as a continuous variable and relate the mean RT to different predictors. In a discrete time survival analysis we redefine our research question from "How is the time-to-event related to different predictors?" to "How is the hazard or risk of event occurrence in each time bin related to different predictors (including the predictor time)?" Discrete-time hazard models allow us to test whether the effect of a predictor on the risk of an event in one or more time periods is statistically significant while controlling for the effects of the other predictors in the model. Predictors can be discrete, continuous, and even time-varying.

The population discrete-time hazard model for object i in time bin j can be written as follows: Cloglog $h(t_{ij}) = [\alpha_1 D_{1ij} + \alpha_2 D_{2ij} + \alpha_3 D_{3ij} + \ldots + \alpha_{10} D_{10ij}] + [\beta_1 X_{1ij} + \beta_2 X_{2ij} + \ldots + \beta_p X_{pij}]$. The main effect of time is modelled using the most flexible specification, that is 10 dichotomous time indicators (D_1 to D_{10}) whose values index the 10 discrete time bins of 2.25 s in this study. The α-parameters multiplied by their respective time indicators represent the baseline cloglog hazard function (i.e., the cloglog hazard value when all predictors are 0). The β-parameters multiplied by their respective predictors represent the (vertical) shift in the baseline cloglog hazard function corresponding to a one unit difference in the associated predictors. So, each β-parameter represents the difference in the population value of cloglog hazard for each unit difference in the predictor while statistically controlling for the effects of all other predictors in the model.

After the parameters of a model are estimated, the fitted cloglog hazard functions can be calculated for specific combinations of values for the predictors. The fitted hazard functions are calculated based on the fitted cloglog hazard functions using the inverse of the cloglog link (hazard = 1 − exp (− exp (cloglog hazard))). Fitted survivor values for each time bin t_j are calculated based on the fitted hazard values $h(t_j)$ as follows: $s(t_j) = [1 - h(t_j)] * [1 - h(t_{j-1})] * \ldots * [1 - h(t_1)]$.

Measurements of predictor variables

The dichotomous predictors included presentation duration (1000 ms and no mask = 0, 150 ms and masked = 1), global symmetry (no = 0, yes = 1),

object category (natural = 0, artifactual = 1), and fragment type (SP = 0, MP = 1).

The continuous predictors based on the closed contour included concept identifiability (a measure of the identifiability of the closed contour based on an independent sample which served as a control for semantic and lexical access; Wagemans et al., 2008), a measure of compactness (i.e., contour length divided by area squared; higher values indicate more circle-like outlines), the number of "strong" extrema or peaks in the outline (i.e., the number of peaks in the curvature graph; determined by the shape-specific adaptive smoothing algorithm of Horng, 2003), and a measure of homogeneity; i.e., the number of peaks divided by area squared). Except for concept identifiability, these continuous predictors were used to assess visual complexity of the closed contour. High complex shapes have a lower compactness, more peaks, and a lower homogeneity compared to low complex shapes. None of these continuous predictors were intercorrelated significantly.

All these predictors were time-invariant (i.e., they had the same value in each time period), but the continuous predictor *proximity* was time-varying because the fragments increased in length. Proximity was measured as the average gap length across each pair of neighbouring contour fragments, which is inversely related to it (Elder & Zucker, 1993). Therefore, given the selected fragmentation levels, it was high for fragmented stimulus versions showing 10% of the contour, and decreased to 0 when fragments grew longer until closure.

RESULTS

Descriptive statistics

Our study counts 12,600 cases (84 participants × 150 stimuli), and the person-period dataset contains 77,185 rows. Overall, correct identification performance was 86% (10,802 times out of 12,600 possible cases). The number of participants (*max* $N = 84$) who identified each object correctly (min = 19; max = 84; mean = 72.01; $SD = 17.07$) is shown in Figure 3a. In Figure 3b, the number of objects (*max* $N = 150$) identified by each participant is presented (min = 77; max = 150; mean = 128.60; $SD = 20.23$).

In Table 1, we present the life table for groups of stimuli presented with or without mask, and differing in object category (natural or artifactual). These life tables summarize the distribution of event occurrence in our sample within the selected groups. The last two columns of each life table display the estimated sample hazard and survivor functions, plotted in Figure 4a and 4b, respectively. Inspection of the overall shape of the estimated hazard

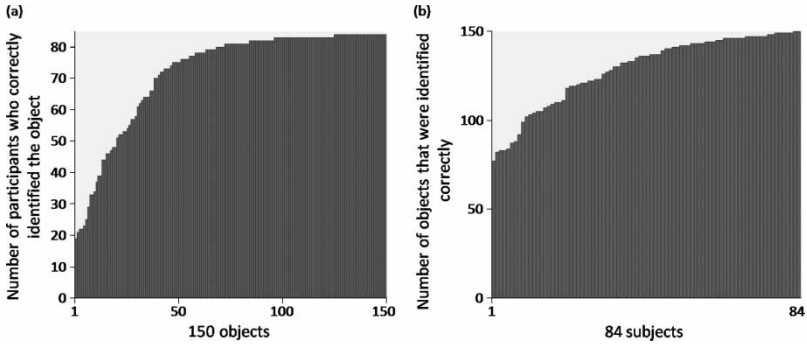

Figure 3. Distribution of the number of objects that were identified correctly by each participant (a), and of the number of participants who identified each object correctly (b).

functions (Figure 4a) shows that the hazard probability of stimuli presented without mask is higher compared to those presented with mask during the first trial. Moreover, this identification advantage for the unmasked condition decreases over time. Also, the hazard probability of natural objects was higher compared to artifactual objects and this difference seems larger for unmasked trials (an interaction between masking and category which might itself evolve in time). The survivor functions in Figure 4b give the probability that a stimulus with certain characteristics is not being identified in each time bin (nor before). When the survivor functions cross the line where the survivor probability equals 0.5, half of those stimuli are estimated to be identified by that time (the median lifetime).

However, to study the strength of these effects while controlling for the effects of the other variables of interest (complexity, symmetry, etc.), we need to fit discrete-time hazard models. Note that we only used modelling as a tool to answer our questions, and not to develop the best-fitting model with the smallest possible number of parameters.

Discrete time hazard models

The GENMOD procedure of SAS 9.1 was used to fit the generalized linear models and estimate the parameters and their standard errors based on generalized estimating equations (GEE; Ballinger, 2004). Besides the percentage concordance, we also implemented the concordance correlation coefficient r_c, and the extended coefficient of determination R^2_m (Zheng, 2000, pp. 1269–1270) as goodness-of-fit (GOF) measures. The model building stage consisted of four stages. We always applied the hierarchical principle (i.e., when a term corresponding to an interaction is included in the

TABLE 1
The life table for four groups of objects (no mask vs. mask, and natural vs. artifactual) including, for each of the ten 2.25 s time bins (Column 1), the number of cases entering the time bin (risk set, Column 2), the number of events (Column 3), and the number of censored observations at the end of the time bin (Column 4)

		No mask					*Mask*				
Object category	*Time bin*	*Risk set*	*No. identified*	*No. censored*	*Hazard*	*Survivor*	*Risk set*	*No. identified*	*No. censored*	*Hazard*	*Survivor*
Natural	1	2772	462	0	.1667	.8333	2772	141	0	.0509	.9491
	2	2310	380	0	.1645	.6962	2631	204	0	.0775	.8755
	3	1930	318	0	.1648	.5815	2427	244	0	.1005	.7875
	4	1612	298	0	.1849	.4740	2183	232	0	.1063	.7038
	5	1314	243	0	.1849	.3864	1951	276	0	.1415	.6043
	6	1071	244	0	.2278	.2983	1675	285	0	.1701	.5014
	7	827	211	0	.2551	.2222	1390	306	0	.2201	.3911
	8	616	185	0	.3003	.1555	1084	305	0	.2814	.2810
	9	431	135	0	.3132	.1068	779	223	0	.2863	.2006
	10	296	116	180	.3919	.0649	556	204	352	.3669	.1270
	Total	13179	2592				17448	2420			

TABLE 1 (*Continued*)

		No mask					*Mask*				
Object category	*Time bin*	*Risk set*	*No. identified*	*No. censored*	*Hazard*	*Survivor*	*Risk set*	*No. identified*	*No. censored*	*Hazard*	*Survivor*
Artifactual	1	3528	363	0	.1029	.8971	3528	104	0	.0295	.9705
	2	3165	309	0	.0976	.8095	3424	152	0	.0444	.9274
	3	2856	274	0	.0959	.7319	3272	195	0	.0596	.8722
	4	2582	291	0	.1127	.6494	3077	245	0	.0796	.8027
	5	2291	322	0	.1405	.5581	2832	277	0	.0978	.7242
	6	1969	347	0	.1762	.4598	2555	315	0	.1233	.6349
	7	1622	322	0	.1985	.3685	2240	362	0	.1616	.5323
	8	1300	283	0	.2177	.2883	1878	380	0	.2023	.4246
	9	1017	251	0	.2468	.2171	1498	340	0	.2270	.3282
	10	766	259	507	.3381	.1437	1158	396	762	.3420	.2160
	Total	21096	3021				25462	2766			

The estimated sample hazard (Column 5) in each time bin equals the number of events divided by the risk set for that time bin. The estimated sample survivor probability in each time bin (Column 6) equals the product of one minus the estimated hazard in that time bin, and the survivor probability in the previous time bin. At Time 0, the survival probability equals 1 and hazard is undefined. The total number of time bins at risk and the total number of events in each group are indicated at the bottom of each table.

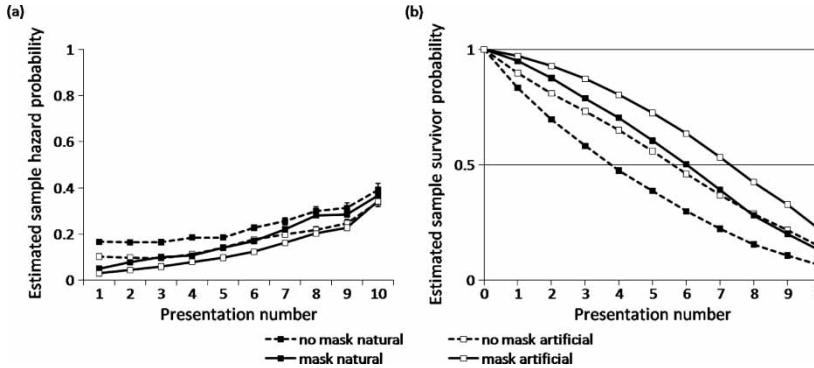

Figure 4. The estimated sample hazard functions (a) and the estimated sample survivor functions (b) based on the data for groups of stimuli which differ in presentation duration (1000 ms and no mask, 150 ms followed by a mask), and object category (natural, artifactual). In this and following figures, presentation number 1 represents time bin]0, 2.25], presentation number 2 time bin]2.25, 4.50], etc.

model, the corresponding lower order terms should also be included; Singer & Willet, 2003).

In Stage 1, we modelled the main effect of time. Both linear and nonlinear effects of time were tested. A linear specification of the main effect of time fitted the cloglog transformed data best (replacing the 10 alphas with $\alpha_0 + \alpha_1$*TIME (TIME is a continuous predictor and was coded as time bin (or presentation number) minus one to centre it on the first time bin). In Stage 2, we included all main effects of the predictors together (15 parameters). The main effect that was least significant (largest *p*-value) was removed, and the reduced model was refitted. This process was repeated until each effect was significant, resulting in the main-effects-only model (see later). In Stage 3, the tenability of the linearity assumption, and the proportionality assumption (i.e., no interactions with time) was evaluated. We investigated interactions between time and each predictor in separate extensions of the main-effects-only model. Note that to test the linearity assumption we divided the range of values of some continuous predictors (i.e., homogeneity, amount of peaks, and compactness) into bins (instead of using polynomial specifications). The reason was that the effects of these continuous predictors could change abruptly when crossing a "threshold value". Fitting the selected specifications for each predictor together generated a nonlinear, nonproportional hazard model (38 parameters). In Stage 4, we evaluated the additivity assumption, by including interactions between predictors. In the final stage of the model building all the possible effects of the predictors (nonlinearity, interactions with time, interactions with other predictors) were included together in one single model (95 parameters). The effect with the largest *p*-value that was not part of any higher order interaction was deleted,

TABLE 2
Parameter estimates for the predictors in the main-effects-only model (in cloglog hazard units), their standard errors, *z*-scores, *p*-values, and GOF measures

Predictor	*Parameter estimate*	*Standard error*	*Z*	*p*
Intercept	−5.7364	0.3944	−1.4540	<.0001
Time	0.2441	0.0092	2.6650	<.0001
Mask	−0.5005	0.0212	2.3600	<.0001
Concept	0.0405	0.0040	1.0150	<.0001
Compact	−4.0292	2.5702	−1.5700	.1170
Proximity	−2.1223	1.1124	−1.9100	.0564

We used a deliberate alpha of .12 for this temporary model. GOF measures: $r_c = .1904$, $R^2_m = .0486$, and Concordance = 56%.

and the reduced model was refitted. This process was repeated until all effects that are not part of any higher order interaction reached significance ($p < .05$), resulting in the final model with 40 parameters (Table 3). We will now discuss the main-effects-only model and the final model in more detail.

The main-effects-only model. The first informative model was the main-effects-only model (Table 2). We report this model to facilitate the interpretation of the parameters in the final model. The main-effects-only model included the linear effect of time, and the main effects of the following predictors: Presentation duration (mask), concept identifiability in the closed contour (concept), compactness of the object (used as a continuous index of complexity), and proximity. This temporary main-effects-only model adheres to the assumptions of proportionality (effects do not vary over time), linearity (a continuous predictor's effect does not depend on the position of the unit difference along its scale), and additivity (the effect of a predictor does not depend on the values of other predictors in the model) for all predictors. Table 2 shows the parameter estimates (in cloglog hazard units), their standard errors, *z*- and *p*-values, and GOF measures.

To illustrate the size of these effects, fitted hazard functions and fitted survivor functions are shown in Figure 5 for hypothetical groups of stimuli with perfect recognition from the closed contour (concept identifiability = 100), but differing in the possible values for presentation duration (unmasked 1000 ms, masked 150 ms), compactness (minimum value in the sample or low compact, maximum value or high compact), and proximity. Since the value of the predictor proximity varies as a function of the object, fragmentation condition (straight vs. curved), and time bin (or contour deletion percentage), the effect of proximity is plotted for two hypothetical (groups of) objects in the same fragmentation condition that differ in the amount of proximity in the first presentation (low, high). Note that for both

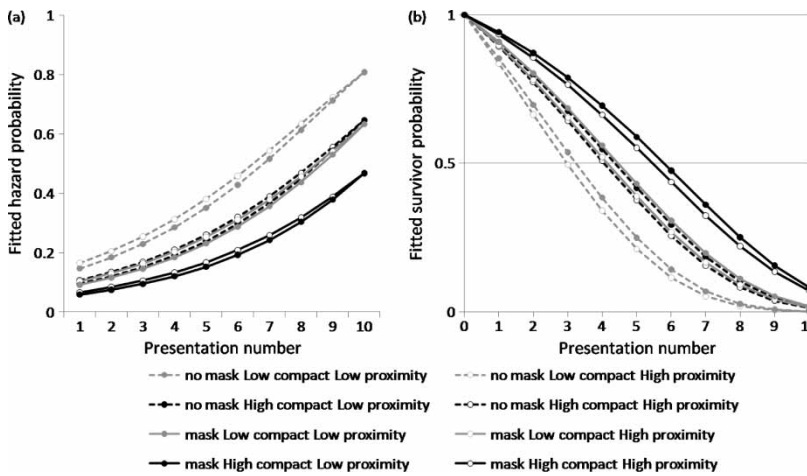

Figure 5. The fitted hazard functions (a) and the fitted survivor functions (b) based on the main-effects-only model for hypothetical groups of stimuli with perfect recognition from the closed contour, but differing in the possible values for presentation duration (1000 ms and no mask; 150 ms and mask), compactness (low compact, high compact), and proximity (low proximity, high proximity).

hypothetical proximity conditions, the average gap length between the fragments gradually decreased to 0 with each presentation or time bin (but faster for low compared to high proximity).

The following effects were significant according to the main-effects-model. First, the main effect of time increased linearly (.2441 in cloglog hazard units, $p < .0001$). (Note that the intercept estimates the cloglog hazard value during the first time period when all other predictors are 0 and should not be interpreted because 0 has no meaning for some continuous predictors). As can be seen in Figure 5a, this linear effect in cloglog units translates to a nonlinear main effect of time in hazard units. This behaviour is the consequence of the (inverse of the) nonlinear cloglog link. This effect of time makes sense because the size of the fragments increases with each presentation number, leading to physical and perceptual closure and a higher (conditional) probability of correct identification. Second, reducing the 1000 ms unmasked presentation duration to a 150 ms masked presentation, lowered the predicted cloglog hazard in each 2.25 s period with 0.5005 cloglog hazard units ($p < .0001$). Exponentiating this parameter indicates that the hazard of correct identification with masking is estimated to be ($e^{-0.5005} =$) .6 times smaller compared to the hazard of correct identification without masking, in each time bin. This is as expected because there is less time to sample from each stimulus when a mask is present. Again note that, although the cloglog hazard functions run parallel, the fitted hazard

functions for the masked and unmasked conditions as shown in Figure 5a do not as a result of the nonlinear cloglog link function. Note how the cloglog hazard value of 0.5005 translates to small differences in hazard when overall hazard is low, and larger differences when overall hazard is high. Third, each unit increase in concept identifiability leads to an increase of 0.0405 cloglog hazard units ($p < .0001$), consistent with improved semantic and lexical access. Fourth, each unit increase in compactness tends to result in a decrease of 4.0292 cloglog hazard units in each time bin ($p = .1170$). Indeed, more compact outlines are more circle-like and less complex, leading to a higher number of activated candidates object representations (Donderi, 2006) and a lower probability of selecting or matching the correct candidate. Finally, each unit increase in average gap length (or unit decrease in proximity) tends to lead to a decrease of 2.1223 cloglog units ($p = .0564$) in each time period.

However, to test our hypotheses, we need to relax the assumptions (proportionality, linearity, and/or additivity) for our predictors. Therefore, we extended the main-effects-only model in separate stages of the model building process (as discussed earlier) resulting in the final model.

The final model. Table 3 shows the 40 parameter estimates of the final nonproportional, nonlinear, and nonadditive model, their standard errors, *z*- and *p*-values, and GOF measures. In Figure 6, we present the fitted hazard functions from the final model for hypothetical groups of stimuli with—for plotting purposes—average values for compactness and the number of peaks, with perfect recognition from the closed contour (concept identifiability = 100), and an average proximity value in time bin 1 with values decreasing across presentations (0 in time bin 10), but differing in presentation duration (1000 ms and no mask or 150 ms and mask), object category (natural or artifactual), global symmetry (symmetrical or asymmetrical), and complexity (low or high homogeneity). Note that we divided the range of values of the continuous variable homogeneity in three classes—low, medium, high—which index high, medium, and low complexity respectively. Also, the values for compactness and number of peaks were each categorized in five classes because it turned out that only high compactness and a low-to-medium number of peaks had significant effects on event occurrence. The corresponding fitted survivor functions are shown in Figure 7.

We will now discuss the effects of each predictor in the final model. We start discussing the main effect of each predictor, which may evolve in time. Afterwards, we discuss the interactions between the predictors, which again may evolve in time. First, consistent with the main-effects-only model, the effect of time on cloglog hazard is primarily a linear increase (Parameter 1,

TABLE 3
Parameter estimates for the predictors in the final model (in cloglog hazard units), their standard errors, *z*-scores, *p*-values, and GOF measures

Predictor		*Parameter estimate*	*Standard error*	*Z*	*p*
1	Intercept	−4.8592	2.1230	−2.2900	.0221
2	Time	0.4728	0.1227	3.8500	.0001
3	Time^2	0.0005	0.0036	0.1500	.8806
4	Mask	−1.6579	0.2529	−6.5600	<.0001
5	Mask*Time	0.1902	0.0311	6.1200	<.0001
6	Mask*Time^2	−.0083	0.0032	−2.5600	.0104
7	Symmetry	0.3766	0.1963	1.9200	.0550
8	Symmetry*Time	−0.0556	0.0215	−2.5800	.0097
9	Artifactual	−0.2633	0.1972	−1.3400	.1818
10	Artifactual*Time	0.0876	0.0210	4.1700	<.0001
11	Low complex	−0.8752	0.2079	−4.2100	<.0001
12	Low complex*Time	0.1152	0.0270	4.2700	<.0001
13	High complex	0.3642	0.2997	1.2200	.2243
14	High complex*Time	0.1015	0.0345	2.9400	.0032
15	Proximity	−2.3404	1.7859	−1.3100	.1900
16	Proximity*Time	0.4879	0.5906	0.8300	.4088
17	Proximity*Time^2	−0.1457	0.0721	−2.0200	.0433
18	No. peaks(2)	−0.6213	0.1716	−3.6200	.0003
19	No. peaks(3)	−0.8719	0.1562	−5.5800	<.0001
20	No. peaks(3)*Time	0.0826	0.0173	4.7900	<.0001
21	Compactness(5)	−0.8915	0.2409	−3.7000	.0002
22	Concept	−0.0140	0.0458	−0.3100	.7601
23	Concept*Time	−0.0036	0.0011	−3.1500	.0016
24	Concept^2	0.0005	0.0003	2.0200	.0432
25	Mask*Symmetry	−0.1511	0.1150	−1.3100	.1889
26	Mask*Symmetry*Time	0.0085	0.0180	0.4700	.6351
27	Mask*Low complex	−0.3569	0.1436	−2.4900	.0129
28	Mask*Low complex*Time	0.0390	0.0231	1.9600	.0916
29	Mask*High complex	−0.2688	0.0899	−2.9900	.0028
30	Mask*Proximity	2.3971	1.0770	2.2300	.0260
31	Mask*Concept	0.0050	0.0024	2.1200	.0339
32	Symmetry*Low complex	0.0986	0.4110	0.2400	.8105
33	Symmetry*Low complex*Time	0.0100	0.0444	0.2300	.8213
34	Symmetry*High complex	−0.0853	0.2288	−0.3700	.7091
35	Artifactual*Low complex	−0.5265	0.1921	−2.7400	.0061
36	Artifactual*High complex	−0.3973	0.3032	−1.3100	.1900
37	Artifactual*High complex*Time	−0.0953	0.0403	−2.3600	.0182
38	Mask*Symmetry*Low complex	0.5715	0.2345	2.4400	.0148
39	Mask*Symmetry*Low complex*Time	−0.0727	0.0346	−2.1000	.0359
40	Mask*Symmetry*High complex	0.4267	0.1209	3.5300	<.0004

Low (high) complex stands for high (low) homogeneity. Numbers between parentheses indicate one of the five classes of values of a categorized continuous variable. For example, Compactness(5) indicates outlines with the highest compactness values. GOF: $r_c = .2242$, $R^2_m = .0912$, and Concordance = 64%

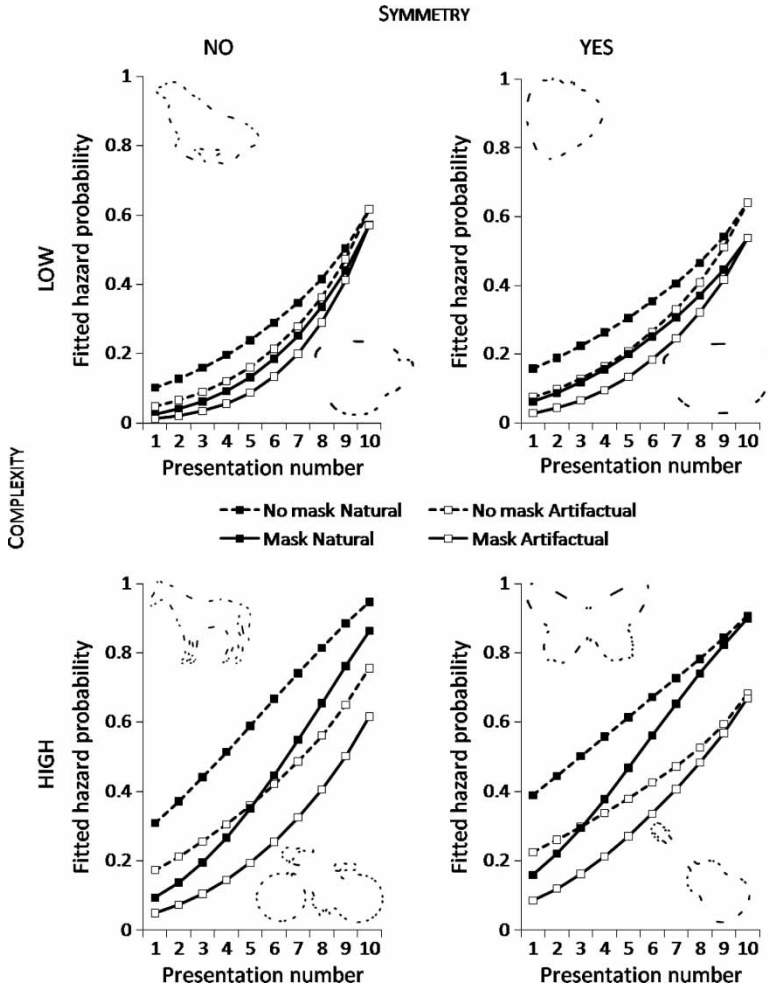

Figure 6. The fitted hazard functions based on the final model for hypothetical groups of stimuli with perfect recognition from the closed contour, and average values for compactness, number of peaks, and proximity. These groups differ on presentation duration (1000 ms and no mask or 150 ms and mask), object category (natural or artifactual), global symmetry (symmetrical or asymmetrical), and complexity (low or high complex). The insets show examples of objects with these specifications (symmetrical or asymmetrical; low or high complex, natural or artifactual). All fragmented object outlines are presented showing 21% of the contour. The fragmentation type of the upper outlines in each of the four graphs is MP; and SP for the lower outlines. Objects are seal, cup, strawberry, bowl, horse, bike, butterfly, and guitar. Note that for reasons of visibility, the insets are thicker than in the actual experiment.

2, and 3). Second, limiting the presentation duration from 1000 to 150 ms (and introducing a mask) leads to a decrease of 1.6579 cloglog hazard units in the first time bin (Parameter 4, $p < .0001$). As suggested by Figure 3, this

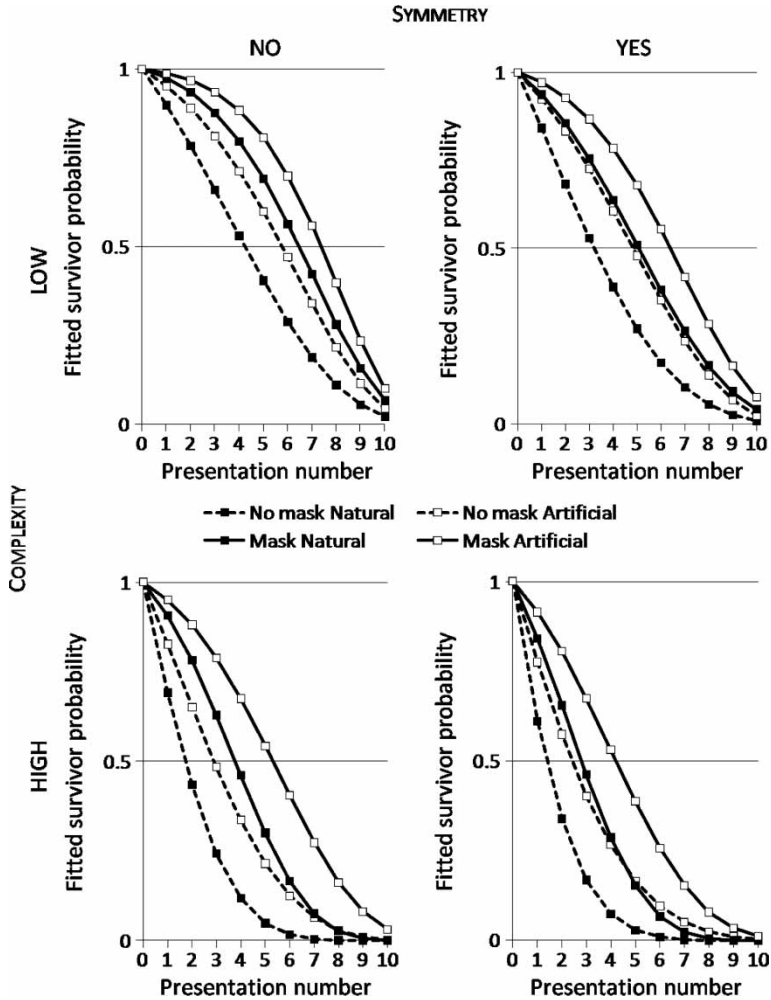

Figure 7. The fitted survivor functions based on the final model for hypothetical groups of stimuli with perfect recognition from the closed contour, and average values for compactness, number of peaks, and proximity. The different groups of stimuli have different values for presentation duration (1000 ms and no mask or 150 ms and mask), object category (natural or artifactual), global symmetry (asymmetrical or symmetrical), and complexity (low or high complex).

disadvantage decreases significantly over time in a quadratic fashion (Parameters 5 and 6). Third, the main advantage for symmetrical compared to asymmetrical objects is almost significant in the first time bin (0.3766 in cloglog hazard units, $p = .0550$; Parameter 7), and this advantage decreased linearly with each subsequent presentation (-0.0556 in cloglog hazard

units, $p = .0097$; Parameter 8). This observation is consistent with the known advantage of symmetry during early perceptual organization (e.g., Machilsen et al., 2009; Wagemans, 1995, 1997), or during the initial activation of a set of possible candidates (Bar, 2003; Donderi, 2006). Fourth, artifactual objects show a nonsignificant main disadvantage compared to natural objects during the first time bin of 0.2633 cloglog hazard units ($p = .1818$; Parameter 9). This disadvantage decreased linearly over time (Parameter 10).

Fifth, the fragmented outlines of objects with a high homogeneity (that is low complex outlines) enjoyed a significant main disadvantage compared to moderately homogeneous (complex) object outlines during the first trial (-0.8752 in cloglog units, $p < .0001$; Parameter 11), and this negative effect decreased linearly over time (0.1152 in cloglog units, $p < .0001$; Parameter 12). This finding is consistent with large initial matching difficulties caused by the activation of many candidate objects for low complex object outlines. On the other hand, highly complex object outlines (with low homogeneity) enjoyed a nonsignificant main advantage compared to moderately complex object outlines in the first time bin (0.3642 in cloglog units, $p = .2243$; Parameter 13), which increased linearly in time (0.1015 in cloglog units, $p = .0032$; Parameter 14). This finding is consistent with efficient matching if initial groupings are correct (Gerlach et al., 2004, 2006). Because the chance of correct grouping increases over time in part due to the increase in fragment length, it is logical that the effect of high complexity increases also. Sixth, similar to the main-effects model, the effect of a unit increase in gap length (or unit decrease in proximity) is to decrease the predicted cloglog hazard with 2.3404 units ($p = .19$; Parameter 15) in the first time bin. This effect increases significantly in a quadratic way (Parameter 17). Interpreting this time-varying main effect of a time-varying predictor is difficult because it depends on the specific object, fragmentation condition, and presentation number. However, broadly speaking, the negative effect stays constant during the first four time bins, after which it increases. Seventh, a rather low number of peaks leads to a predicted decrease of 0.6213 cloglog hazard units in each time interval ($p < .001$; Parameter 18). Also, contours with an average number of peaks leads to a predicted decrease of 0.8719 cloglog hazard units in the first time interval ($p < .001$; Parameter 19); this negative effect decreases over time (Parameter 20). Eight, contours with the highest compactness values or, in other words, the most circle-like ones enjoy a disadvantage of 0.8915 cloglog hazard units in each trial ($p < .001$; Parameter 21). These latter effects are consistent with the idea that low visual complexity (low-to-medium number of peaks and/or high compactness) leads to matching difficulties due to the many activated candidates. Finally, the effect of

concept is positive in the first trial and decreases linearly over time (Parameters 22, 23, and 24).[1]

We now discuss the interactions between predictors (and possibly time). First, the predictor mask was involved in one-way interactions with homogeneity (or complexity) (Parameters 27–29), with proximity (Parameter 30), and with concept (Parameter 31). Masking low complex objects resulted in an additional decrease in identification probability of 0.3569 cloglog hazard units during the first time bin ($p = .0129$; Parameter 27); this effect tended to decrease linearly over time ($p = .0916$; Parameter 28). Masking high complex objects also resulted in an additional decrease in identification performance in every time bin of 0.2688 cloglog hazard units ($p = .0028$; Parameter 29). When masked, there was an additional effect of proximity of 2.3971 cloglog hazard units in each time bin ($p = .026$; Parameter 30). Because this parameter is in absolute terms as large as Pparameter 15 (the negative main effect of proximity in the first time bin), this observation suggests that there is no effect of proximity in the first (few) time bins of the masked conditions.

Mask also interacted with concept ($p = .0339$; Parameter 31). This shows that each unit increase in concept identifiability under masked conditions, leads to an additional increase in identification performance of 0.005 cloglog hazard units in each trial. Although this value is small, a speculative explanation is that a long, unmasked presentation duration of 1000 ms allows the activation of more irrelevant candidate objects, compared to a short masked presentation duration of 150 ms.

Moreover, category interacted with homogeneity or complexity (Parameters 35–37). If the outline was low complex (high homogeneity) and the object artifactual, then there was an additional identification disadvantage of 0.5265 cloglog hazard units in each time bin ($p < .01$; Parameter 35). If the outline was high complex (low homogeneity) and the object an artifact, then there was a nonsignificant additional identification disadvantage of 0.3973 cloglog hazard units in the first time bin ($p = .19$; Parameter 36) which increased in a linear way over time ($p = .0182$; Parameter 37). Finally, there were two-way interactions between mask, symmetry, and homogeneity or complexity (Parameters 38–40). Note that the one-way interactions that are part of these two-way interactions (i.e., Parameters 25, 26, 32, 33, and 34) were not significant. If low complex (high homogeneity) and masked stimuli were symmetrical, there was a significant identification advantage during the first time bin of 0.5715 cloglog hazard units ($p = .0148$; Parameter 38); this effect decreased linearly over time (Parameter 39). If high complex and

[1] For example, for a concept value of 100 the predicted effect of a unit increase in concept in the first 2.25 s time bin equals 100 times -0.014 (Parameter 22) $+100$ times 0 times -0.0036 (Parameter 23) $+100$ times 100 times 0.0005 (Parameter 24) $=3.6$ cloglog hazard units.

masked stimuli were symmetrical, there was a significant advantage during every time bin of 0.4267 cloglog hazard units ($p < .001$; Parameter 40).

DISCUSSION

To study the possibly interactive and concurrent effects of variables like exposure duration (1000 ms vs. 150 ms), fragment curvature (low vs. high), contour integration cues (local proximity, global symmetry), stimulus complexity, and object category (natural vs. artifactual) on grouping and matching processes during identification of fragmented object outlines, we used a dynamic build-up paradigm with fragments increasing in length in 10 steps every 2.25 s, and recorded the lowest presentation number that resulted in correct basic-level naming by the participants.

The results: (1) Are consistent with many predictions from the literature, (2) extend the results of Panis and Wagemans (2009), and (3) suggest that our identification paradigm and analysis method can be useful for studying processing differences between normals and patient populations, or between adults and children.

First, the observed main effects of complexity, symmetry, and category are consistent with predictions from the literature. Low complex objects (highly homogeneous) show a decreasing disadvantage compared to medium complex objects because of an initial matching disadvantage, whereas high complex objects (low homogeneity) show an increasing advantage (Parameters 11–14). This difference between low and high complexity as indexed by homogeneity is more or less constant over time given the same values for the linear change in time of the effects of low and high homogeneity (Parameters 12 and 14). Note that Panis and Wagemans (2009) found a constant negative main effect of low complexity, and a decreasing advantage for high complexity using repetitions of the same fragmentation level (20%).

The positive effect of the global configural property symmetry is highest during the first presentation and decreases over time (Parameters 7 and 8). Furthermore, with short masked presentations there is an extra positive effect of symmetry, which decreases over time for low complex objects (Parameters 38, 39, and 40). This early positive effect of symmetry is consistent with a grouping advantage (Machilsen et al., 2009; Wagemans, 1995, 1997) or with a smaller set of activated candidates (only symmetrical candidates).

Interestingly, with masking, the effect of proximity was eliminated in the first (few) time bin(s). This observation suggest that relating the neighbouring fragments along the contour takes more time compared to extracting more global configural relations between fragments across the whole image. Together with the fact that the effect of a local fragment property like

fragment curvature was not significant, these observations are consistent with the dominance of global configural properties during early grouping processes, compared to local fragment properties (fragment curvature) or more local configural properties (proximity), as found by Panis and Wagemans (2009).

Fragmented outlines of natural objects enjoy an identification advantage compared to artifactual objects (Parameters 11, 12, 35, 36, 37). According to (Gerlach et al. 2002, 2004, 2006) this advantage for natural objects is resulting from a more efficient top-down guidance in the grouping of the fragments due to their higher structural similarity compared to artifactual objects. Indeed, the identification disadvantage for artifacts in the first time bin increased over time when the object was complex (Parameter 37). As can be seen in the lower panels of Figure 6, this effect resulted in a crossing of the hazard functions for unmasked artifacts and masked natural objects (earlier for symmetric outlines compared to asymmetric outlines). Thus, while the hazard for masked natural objects is initially lower compared to hazard for masked natural objects, with time the hazard for masked natural objects becomes larger than the hazard for unmasked artifactual objects. This is consistent with a more efficient top-down guidance for grouping fragments of natural objects (and more efficient for symmetrical compared to asymmetrical outlines).

Second, our results extend those of Panis and Wagemans (2009). By manipulating the exposure duration between participants, we found that limiting the presentation time and introducing a mask had a negative effect on identification hazard in the first time bin which decreased over time (Parameters 4, 5, and 6). Furthermore, the effect of mask interacted with complexity (next to proximity and concept). With 150 ms masked presentation durations, there was an extra disadvantage to identify low and high complex objects (Parameters 27 and 29). However, this negative effect of masking was eliminated when symmetry was present (Parameters 27 vs. 38, and 29 vs. 40). In other words, the positive effect of symmetry is larger than the negative effect of masking, suggesting that symmetry information can be detected within 150 ms. On a more speculative note, the interactions between mask and proximity, and between mask and concept suggest that compared to a 150 ms masked presentation, an unmasked 1000 ms presentation allows more grouping of neighbouring fragments along the contour, and the activation of more irrelevant object candidates or interpretations.

In the current study, all the hazard functions increased with time. This was not the case for the data of Panis and Wagemans (2009), who found that hazard functions eventually decreased after an initial increase, especially for high complex shapes. The reason is obvious. Panis and Wagemans used fragmented outlines with 20% of the contour shown at each presentation time, and lengthened the presentation duration gradually with each extra

identification attempt required; here we let the percentage of the contour shown increase from 10, to 12, 16, 21, 27, ... 100%, and we used a constant presentation duration. This procedural difference resulted in (1) more correct identifications in the current study with the passage of time, and (2) a possible tendency of the participants to wait longer before outputting their response because they could evaluate their initial guess based on more information in the next presentations.

One important difference with the results of Panis and Wagemans (2009) is that the current study failed to find any effect of the curvature of the fragments. Probably, the reason is that the difference between curved and straight fragments disappears rather quickly in the stimuli when the fragments increase in length. A possible tendency to wait for longer contour fragments before deciding on a response would also lead to an inability to find significant effects of fragment curvature. Note that during the exploratory analyses, we did observe small advantages for straight fragments compared to curved ones for complex objects during the first few presentation times (consistent with Panis & Wagemans). However, we never observed the late advantage for curved fragments compared to straight ones for low complex objects as Panis and Wagemans did. In their study, the size of the fragments did not change with each presentation, only the presentation time.

Third, our identification paradigm and analysis method can be useful for studying processing differences between normals and patient populations, or between adults and children. The dynamic build-up paradigm ensures that overall identification performance is high since the closed contour is shown if necessary. This property makes this paradigm attractive when testing children or patient populations that have motivational problems. In general, the abilities of the participants should determine the tradeoff between the number of trials per subject and the number of subjects in the study.

The use of survival analysis allows quantifying processing differences between adults and children, or between normals and patient populations. For example, patients with autism differ from normals in their perceptual processing (evidence reviewed by Dakin & Frith, 2005). A first difference—superior processing of fine detail (local structure)—is fairly well established, but a second difference—inferior processing of global structure (or impaired contextual processing)—is less well established because experimental studies have not precluded observers using more local cues. Using survival analysis, one can investigate whether the effects of local detail (e.g., fragment curvature) and global structure (e.g., symmetry) change differently over time for autism patients compared to normals. Also, people with frontal lobe damage, simultanagnosia, or integrative agnosia might show different effects of, for example, object complexity. Note that certain perceptual deficiencies might only become evident using systematically degraded stimuli (Sadr &

Sinha, 2004). Contour deletion is not the only technique to degrade images. For example, in the Random Image Structure Evolution technique (RISE paradigm), the spatial structure of intact pictures is gradually degraded by scrambling the phase spectrum (Sadr & Sinha, 2004), and the bubble technique introduces randomly positioned (Gaussian) "windows" across an image to study which image features drive a measurable response (Gosselin & Schyns, 2001).

Finally, we offer recommendations for future studies using fragmented object outlines. If the research questions concerns at least local fragment properties such as fragment curvature, length, and position, we suggest using a single fragmentation level as in Panis and Wagemans (2009) with either constant or increasing presentation durations. On the other hand, if the task must be made easier or more rewarding because one is dealing with patients or children, and interest lies mainly in global or configural properties (symmetry, complexity) or memory (category), we suggest to use the current dynamic build-up paradigm.

CONCLUSION

Disentangling the concurrent effects of variables like symmetry, object category, complexity, fragment curvature, etc. on the grouping and matching processes during identification is possible using the well-established technique of survival analysis. Our stimuli and paradigm seem well suited to study temporal processing advantages or disadvantages in children and patient populations compared to normals.

REFERENCES

Allison, P. D. (1982). Discrete-time methods for the analysis of event histories. *Sociological Methodology*, *13*, 61–98.

Attneave, F. (1954). Some informational aspects of visual perception. *Psychological Review*, *61*, 183–193.

Ballinger, G. A. (2004). Using generalized estimating equations for longitudinal data analysis. *Organizational Research Methods*, *7*, 127–150.

Bar, M. (2003). A cortical mechanism for triggering top-down facilitation in visual object recognition. *Journal of Cognitive Neuroscience*, *15*, 600–609.

Bar, M., Kassam, K. S., Ghuman, A. S., Boshyan, J., Schmid, A. M., Dale, A. M., et al. (2006). Top-down facilitation of visual recognition. *Proceedings of the National Academy of Sciences of the USA*, *103*, 449–454.

Biederman, I. (1987). Recognition-by-components: A theory of human image understanding. *Psychological Review*, *94*, 115–147.

Dakin, S., & Frith, U. (2005). Vagaries of visual perception in autism. *Neuron*, *48*, 497–507.

De Winter, J., & Wagemans, J. (2004). Contour-based object identification and segmentation: Stimuli, norms and data, and software tools. *Behaviour Research Methods, Instruments, and Computers*, *36*, 604–624.

De Winter, J., & Wagemans, J. (2006). Segmentation of object outlines into parts: A large scale integrative study. *Cognition*, *99*, 275–325.

De Winter, J., & Wagemans, J. (2008a). Perceptual saliency of points along the contour of everyday objects: A large-scale study. *Perception and Psychophysics*, *70*, 50–64.

De Winter, J., & Wagemans, J. (2008b). The awakening of Attneave's sleeping cat: Identification of everyday objects on the basis of straight-line segments. *Perception*, *37*, 245–270.

Donderi, D. C. (2006). Visual complexity: A review. *Psychological Bulletin*, *132*, 73–97.

Elder, J., & Zucker, S. (1993). The effect of contour closure on the rapid discrimination of two-dimensional shapes. *Vision Research*, *33*, 981–991.

Feldman, J., & Singh, M. (2005). Information along contours and object boundaries. *Psychological Review*, *112*, 243–252.

Gerlach, C., Aaside, C. T., Humphreys, G. W., Gade, A., Paulson, O. B., & Law, I. (2002). Brain activity related to integrative processes in visual object recognition: Bottom-up integration and the modulatory influence of stored knowledge. *Neuropsychologia*, *40*, 1254–1267.

Gerlach, C., Law, I., & Paulson, O. B. (2004). Structural similarity and category-specificity: A refined account. *Neuropsychologia*, *42*, 1543–1553.

Gerlach, C., Law, I., & Paulson, O. B. (2006). Shape configuration and category-specificity. *Neuropsychologia*, *44*, 1247–1260.

Gosselin, F., & Schyns, P. G. (2001). Bubbles: A technique to reveal the use of information in recognition tasks. *Vision Research*, *41*, 2261–2271.

Hochstein, S., & Ahissar, M. (2002). View from the top: Hierarchies and reverse hierarchies in the visual system. *Neuron*, *36*, 791–804.

Horng, J.-H. (2003). An adaptive smoothing approach for fitting digital planar curves with line segments and circular arcs. *Pattern Recognition Letters*, *24*, 565–577.

Humphreys, G. W., & Forde, E. M. E. (2001). Hierarchies, similarity, and interactivity in object recognition: "Category-specific" neuropsychological deficits. *Behavioural and Brain Sciences*, *24*, 453–509.

Humphreys, G. W., Riddoch, M. J., & Quinlan, P. T. (1988). Cascade processes in picture identification. *Cognitive Neuropsychology*, *5*, 67–103.

Kennedy, J. M., & Domander, R. (1985). Shape and contour: The points of maximum change are least useful for recognition. *Perception*, *14*, 367–370.

Kimchi, R., & Bloch, B. (1998). Dominance of configural properties in visual form perception. *Psychonomic Bulletin and Review*, *5*, 135–139.

Kimchi, R., & Hadad, B.-S. (2002). Influence of past experience on perceptual grouping. *Psychological Science*, *13*, 41–47.

Kosslyn, S. M., Alpert, N. M., Thompson, W. L., Chabris, C. F., Rauch, S. L., & Anderson, A K. (1994). Identifying objects seen from different viewpoints: A PET investigation. *Brain*, *117*, 1055–1071.

Kveraga, K., Boshyan, J., & Bar, M. (2007). Magnocellular projections as the trigger of top-down facilitation in recognition. *Journal of Neuroscience*, *27*, 13232–13240.

Lamme, V. A. F., Supèr, H., & Spekreijse, H. (1998). Feedforward, horizontal, and feedback processing in the visual cortex. *Current Opinion in Neurobiology*, *8*, 529–535.

Liu, Z., Jacobs, D. W., & Basri, R. (1999). The role of convexity in perceptual completion: Beyond good continuation. *Vision Research*, *39*, 4244–4257.

Lloyd-Jones, T. J., & Luckhurst, L. (2002). Outline shape is a mediator of object recognition that is particularly important for living things. *Memory and Cognition*, *30*, 489–498.

Locher, P., & Wagemans, J. (1993). The effects of element type and spatial grouping on symmetry detection. *Perception*, *22*, 565–587.

Luce, R. D. (1986). *Response times: Their role in inferring elementary mental organization*. New York: Oxford University Press.

Machilsen, B., Pauwels, M., & Wagemans, J. (2009). The role of vertical mirror-symmetry in visual shape detection. *Journal of Vision*, *9*(12), art. 11, 1–11. doi: 10.1167/9.12.11 http://journalofvision.org/9/12/11/

Murray, S. O., Schrater, P., & Kersten, D. (2004). Perceptual grouping and the interactions between visual cortical areas. *Neural Networks*, *17*, 695–705.

Norman, J. F., Philips, F., & Ross, H. E. (2001). Information concentration along the boundary contours of naturally shaped solid objects. *Perception*, *30*, 1285–1294.

Nucci, M., & Wagemans, J. (2007). Goodness of regularity in dot patterns: Global symmetry, local symmetry and their interactions. *Perception*, *36*, 1305–1319.

Panis, S., de Winter, J., Vandekerckhove, J., & Wagemans, J. (2008). Identification of everyday objects on the basis of fragmented outline versions. *Perception*, *37*, 271–289.

Panis, S., & Wagemans, J. (2009). Time-course contingencies in perceptual organization and object identification of fragmented object outlines. *Journal of Experimental Psychology: Human Perception and Performance*, *35*(3), 661–687.

Panis, S., & Wagemans, J. (2010). Using discrete time hazard modelling to study the timing of behaviour. *Manuscript submitted for publication*.

Riddoch, M. J., & Humphreys, G. W. (2004). Object identification in simultanagnosia: When wholes are not the sum of their parts. *Cognitive Neuropsychology*, *21*, 423–441.

Sadr, J., & Sinha, P. (2004). Object recognition and Random Image Structure Evolution. *Cognitive Science*, *28*, 259–287.

Sanocki, T. (1993). Time course of object identification: Evidence for a global-to-local contingency. *Journal of Experimental Psychology: Human Perception and Performance*, *19*, 878–898.

Sanocki, T. (2001). Interaction of scale and time during object identification. *Journal of Experimental Psychology: Human Perception and Performance*, *27*, 290–302.

Schendan, H. E., & Kutas, M. (2002). Neurophysiological evidence for two processing times for visual object identification. *Neuropsychologia*, *40*, 931–945.

Schendan, H. E., & Kutas, M. (2007). Neurophysiological evidence for the time course of activation of global shape, part, and local contour representations during visual object categorization and memory. *Journal of Cognitive Neurosciences*, *19*, 734–749.

Sekuler, A. B., Palmer, S. E., & Flynn, C. (1994). Local and global processes in visual completion. *Psychological Science*, *5*, 260–267.

Severens, E., van Lommel, S., Ratinckx, E., & Hartsuiker, R. J. (2005). Timed picture naming norms for 590 pictures in Dutch. *Acta Psychologica*, *119*, 159–187.

Singer, J. D., & Willett, J. B. (1993). It's about time: Using discrete-time survival analysis to study duration and the timing of events. *Journal of Educational Statistics*, *18*, 155–195.

Singer, J. D., & Wilett, J. B. (2003). *Applied longitudinal data analysis: Modeling change and event occurrence*. New York: Oxford University Press.

Singh, M., & Fulvio, J. M. (2005). Visual extrapolation of contour geometry. *Proceedings of the National Academy of Sciences of the USA*, *102*, 939–944.

Snodgrass, J. G., & Corwin, J. (1988). Perceptual identification thresholds for 150 fragmented pictures from the Snodgrass and Vanderwart picture set. *Perceptual and Motor Skills*, *67*, 3–36.

Snodgrass, J. G., & Vanderwart, M. (1980). A standardized set of 260 pictures: Norms for name agreement, image agreement, familiarity, and visual complexity. *Journal of Experimental Psychology: Human Learning and Memory*, *6*, 174–215.

Spillman, L. (1999). From elements to perception: Local and global processing in visual neurons. *Perception*, *28*, 1461–1492.

Sugase, Y., Yamane, S., Ueno, S., & Kawano, K. (1999). Global and fine information coded by single neurons in the temporal visual cortex. *Nature*, *400*, 869–873.

Tomita, H., Ohbayashi, M., Nakahara, K., Hasegawa, I., & Miyashita, Y. (1999). Top-down signal from prefrontal cortex in executive control of memory retrieval. *Nature*, *401*, 699–703.

Wagemans, J. (1992). Perceptual use of nonaccidental properties. *Canadian Journal of Psychology*, *46*, 236–279.

Wagemans, J. (1993). Skewed symmetry: A nonaccidental property used to perceive visual forms. *Journal of Experimental Psychology: Human Perception and Performance*, *19*, 364–380.

Wagemans, J. (1995). Detection of visual symmetries. *Spatial Vision*, *9*, 9–32.

Wagemans, J. (1997). Characteristics and models of human symmetry detection. *Trends in Cognitive Sciences*, *1*, 346–352.

Wagemans, J., de Winter, J., Op de Beeck, H., Ploeger, A., Beckers, T., & Vanroose, P. (2008). Identification of everyday objects on the basis of silhouette and outline versions. *Perception*, *37*, 207–244.

Wagemans, J., Notebaert, W., & Boucart, M. (1998). Lorazepam but not diazepam impairs identification of pictures on the basis of specific contour fragments. *Psychopharmacology*, *138*, 326–333.

Zheng, B. (2000). Summarizing the goodness of fit of generalized linear models for longitudinal data. *Statistics in Medicine*, *19*, 1265–1275.

Manuscript received July 2009
Manuscript accepted November 2009
First published online July 2010